Available online at www.sciencedirect.com
ScienceDirect
Trans. Nonferrous Met. Soc. China 23(2013) 2201−2208
Transactions of Nonferrous Metals Society of China
www.tnmsc.cn

Optimization model of GNSS/pseudolites structure design for open-pit mine positioning

Zheng-ying SHAN[1], Hou-zeng HAN[2], Kun JIANG[2]

1. College of Civil Engineering, Chongqing University, Chongqing 400030, China;
2. National Administration of Surveying, Mapping and Geoinformation (NASG) Key Laboratory for Land Environment and Disaster Monitoring, China University of Mining and Technology, Xuzhou 221116, China

Received 11 December 2012; accepted 8 January 2013

Abstract: A new pseudolites (PLs) structure optimization model of global navigation satellite system (GNSS)/PLs integration positioning system used in deep open-pit mine was presented. Position dilution of precision ($P_{\rm dop}$) and reliability were selected as the optimization indicators to build a multi-objective optimization model to decide the optimum PLs location. A scheme was designed by establishing a four-dimensional model taking azimuth (a), elevation angle (e) and epoch (t) of satellites as the input independent variables and $P_{\rm dop}$ as the dependent variable to calculate the optimum PLs location zone considering the real circumstances. And then the ultimate PLs location can be fixed by testing the curves of $P_{\rm dop}$ along time. A field collected Trimble R8 GPS data set in China University of Mining and Technology (CUMT) campus was used for the model test to show the effectiveness, and the proposed PLs optimum design scheme was used at the west open-pit mine of Fushun mining group Co., Ltd., in China, better $P_{\rm dop}$ and reliability have been achieved for the integration system. Both experiments show that the proposed scheme is excellent in designing GNSS/PLs system which is helpful for improving the performance of the positioning system and reducing the cost.

Key words: open-pit mine; dilution of precision; reliability; GNSS/PLs system; optimization

1 Introduction

Location based application plays an important role in open-pit mining. Traditional positioning strategies like total station surveying and leveling are susceptible to the circumstances and labor-intensive [1,2]. The global navigation satellite system (GNSS) is a new positioning technique and the services are available all over the world for all 24 h with high precision, which is widely used in open-pit mine vehicle dispatching, equipment monitoring and landslide hazard monitoring [3−6]. However, the slopes of deep open-pit mines probably reduce the GNSS satellite visibility, which leads to low precision and unreliable positioning results. Therefore, some augmentation systems are required to increase the accuracy, availability and reliability of the GNSS.

Several augmented systems have been integrated into the current GNSS system. The WIFI wireless location technology was proposed for the open-pit mine positioning and dispatching for relatively low precision positioning application [7]. Pseudolites(PLs) positioning system, which has obvious advantages on extremely low elevation angle, can avoid the GNSS constellation problems of bad satellites distribution and poor signal strength used in open-pit mine and the GNSS/PLs integration system is another selection for cm-level positioning applications [8]. The positioning system is a typical PLs based positioning system already used in mine, in urban canyon and emergency life-saving area [9].

For GNSS/PLs integration system, the number and position of PLs used should be determined based on several simulation experiments or by comparing with existing PLs application cases [10,11]. Unfortunately, there are still not theory analysis and optimal strategy for PLs number determination and location optimization.

In the present work, a PLs optimal design scheme was proposed based on multi-objective optimization model for designing PLs number and location of a GNSS/PLs integration positioning system used in open-pit mine. The practical design at the west open-pit

Foundation item: Project (2013RC16) supported by the Fundamental Research Funds for the Central Universities, China
Corresponding author: Hou-zeng HAN; Tel: +86-15162116282; E-mail: houzeng_han@163.com
DOI: 10.1016/S1003-6326(13)62718-1

mine of Fushun mining group Co., Ltd., in China shows satisfactory performance.

2 Dilution of precision

Dilution of precision (D_{op}) is a term used in GNSS to specify the additional multiplicative effect of GPS satellite geometry on GPS precision. This work uses it to evaluate the system performance of the PLs augmented GNSS.

If absolute range measurements are available and the receiver is synchronized with the base stations [12], the range from the receiver to the ith satellite is:

$$R_i=\sqrt{(x-x_i)^2+(y-y_i)^2+(z-z_i)^2} \tag{1}$$

where (x_i, y_i, z_i) is the coordinate of the ith satellite. Then linear combination observation ΔR_i can be given as

$$\Delta R_i=\sqrt{(x-x_1)^2+(y-y_1)^2+(z-z_1)^2}-\sqrt{(x-x_i)^2+(y-y_i)^2+(z-z_i)^2} \tag{2}$$

Taylor's theorem is normally applied to linearizing Eq. (2) and we have

$$\boldsymbol{H}\Delta\boldsymbol{x}=\Delta\boldsymbol{r} \tag{3}$$

where $\Delta\boldsymbol{x}$ is the vector offset of the true position of the receiver from the linearization point; $\Delta\boldsymbol{r}$ is the difference of the true range and the computed range corresponding to the nominal point; and $\boldsymbol{H}$ can be represented as

$$\boldsymbol{H}=\begin{bmatrix} \frac{x-x_1}{R_1}-\frac{x-x_2}{R_2} & \frac{y-y_1}{R_1}-\frac{y-y_2}{R_2} & \frac{z-z_1}{R_1}-\frac{z-z_2}{R_2} \\ \vdots & \vdots & \vdots \\ \frac{x-x_1}{R_1}-\frac{x-x_n}{R_n} & \frac{y-y_1}{R_1}-\frac{y-y_n}{R_n} & \frac{z-z_1}{R_1}-\frac{z-z_n}{R_n} \end{bmatrix} \tag{4}$$

And the vector offset is solved according to least square (LS) as

$$\Delta\boldsymbol{x}=(\boldsymbol{H}^{\mathrm{T}}\boldsymbol{H})^{-1}\boldsymbol{H}^{\mathrm{T}}\Delta\boldsymbol{r} \tag{5}$$

It can also be expressed as

$$d\boldsymbol{x}=(\boldsymbol{H}^{\mathrm{T}}\boldsymbol{Q}^{-1}\boldsymbol{H})^{-1}\boldsymbol{H}^{\mathrm{T}}\mathrm{d}\boldsymbol{r} \tag{6}$$

where $\boldsymbol{Q}$ is the error covariance matrix of observations.

Then, D_{op} is defined as

$$D_{op}=\frac{\sigma_x}{\sigma_y} \tag{7}$$

And

$$\mathrm{cov}(\mathrm{d}\boldsymbol{x})=E(\mathrm{d}\boldsymbol{x}\mathrm{d}\boldsymbol{x}^{\mathrm{T}})=E[(\boldsymbol{H}^{\mathrm{T}}\boldsymbol{H})^{-1}]\boldsymbol{H}^{\mathrm{T}}\mathrm{d}\boldsymbol{r}\mathrm{d}\boldsymbol{r}^{\mathrm{T}}\boldsymbol{H}(\boldsymbol{H}^{\mathrm{T}}\boldsymbol{H})^{-1}$$
$$=(\boldsymbol{H}^{\mathrm{T}}\boldsymbol{H})^{-1}\boldsymbol{H}^{\mathrm{T}}\mathrm{cov}(\mathrm{d}\boldsymbol{r})\boldsymbol{H}(\boldsymbol{H}^{\mathrm{T}}\boldsymbol{H})^{-1}=(\boldsymbol{H}^{\mathrm{T}}\boldsymbol{H})^{-1}\sigma_r^2$$

$$P_{dop}=\frac{\sqrt{\sigma_x^2+\sigma_y^2+\sigma_z^2}}{\sigma_r}$$
$$=\sqrt{((\boldsymbol{H}^T\boldsymbol{H})^{-1})_{1,1}+(\boldsymbol{H}^T\boldsymbol{H})^{-1})_{2,2}+((\boldsymbol{H}^T\boldsymbol{H})^{-1})_{3,3}} \tag{8}$$

It is shown that P_{dop} is only related to the satellites distribution with respect to a specific receiver.

3 Reliability

Reliability is applied to evaluating the system's ability to detect outliers and assess the impact of undetectable outliers on the navigation solution. The linearized GNSS position equation is

$$\boldsymbol{l}=\boldsymbol{Ax}+v \tag{9}$$

where $\boldsymbol{A}$ is the design matrix of the error equations; v represents the residuals; the observations $\boldsymbol{l}$ are used to estimate the parameters $\boldsymbol{x}$. The unknowns and the residuals are estimated using the weighted least square (WLS):

$$\hat{\boldsymbol{x}}=(\boldsymbol{A}^{\mathrm{T}}\boldsymbol{PA})^{-1}\boldsymbol{A}^{\mathrm{T}}\boldsymbol{Pl} \tag{10}$$

$$\hat{\boldsymbol{v}}=\boldsymbol{A}\hat{\boldsymbol{x}}-\boldsymbol{l}=(\boldsymbol{A}(\boldsymbol{A}^{\mathrm{T}}\boldsymbol{PA})^{-1}\boldsymbol{A}^{\mathrm{T}}\boldsymbol{P}-\boldsymbol{I})\boldsymbol{l} \tag{11}$$

where $\hat{\boldsymbol{x}}$ is the estimated unknown; $\hat{\boldsymbol{v}}$ is the residuals; and $\boldsymbol{P}$ is the weight matrix of the measurements. The corresponding variance covariance matrix of the residuals can be expressed as

$$\boldsymbol{Q}_{\hat{v}}=P^{-1}-\boldsymbol{A}(\boldsymbol{A}^{\mathrm{T}}\boldsymbol{PA})^{-1}\boldsymbol{A}^{\mathrm{T}} \tag{12}$$

The measure of internal reliability is quantified as the minimal detectable bias (M_{DB}). For a given level of confidence and related observations, M_{DB} is [13]

$$M_{\mathrm{DB},i}=\frac{\delta_0}{\sqrt{\boldsymbol{e}_i^{\mathrm{T}}\boldsymbol{PQ}_{\hat{v}}\boldsymbol{Pe}_i}} \tag{13}$$

where $\boldsymbol{e}_i$ is a unit vector in which the ith element has a value equal to one; δ_0 is a non-centrality parameter of w-test for gross error inspection and

$$\delta_0=N_{1-\alpha_0/2}(0,1)+N_{1-\beta_0}(0,1) \tag{14}$$

where α_0 is the alarm rate and β_0 is the detectability.

For a reliable system, the corresponding internal reliability r_i should meet

$$c_i\le r_i\le d_i$$

where c_i and d_i are both positive integers. if $\max\{\inf(r_i)\}<\min(c_i)$, then the system is regarded as unreliable.

The influence of the undetected error on the estimated parameters is called external reliability. External reliability measures are evaluated as [11,14]

$$\nabla_{0,\hat{x}}=\boldsymbol{Q}_{\hat{x}}\boldsymbol{A}^{\mathrm{T}}\boldsymbol{Pe}_i\nabla_0\boldsymbol{s}_i \tag{15}$$

where $\boldsymbol{Q}_{\hat{x}}$ is the 'a posteriori' variance covariance matrix of the estimated parameters.

4 Design on PLs structure optimization

4.1 Theoretical basis

Several constraint conditions are selected to design the PLs structure with objective optimization model. Usually, single objective optimization design only focuses on precision or reliability. It lacks the consideration on all constraints [15]. We hope that our optimization scheme contains several objective functions. However, the conditions may not be optimal simultaneously for all the criteria and an optimal design that satisfies all constraints may not exist. This work adopted a comprehensive assessment function by coordinating different objective functions with different weight coefficients [16,17].

Let f_1^*, f_2^* and f_3^* be the optimal design conditions of precision, reliability and cost respectively , then the objective constraints are

$$\begin{cases} f_1(\boldsymbol{P}_1,\ \boldsymbol{P}_2,\ \cdots,\ \boldsymbol{P}_n)=\boldsymbol{a}^{\mathrm{T}}(\boldsymbol{A}^{\mathrm{T}}\boldsymbol{PA})^{-1}\boldsymbol{a} \\ f_2(\boldsymbol{P}_1,\boldsymbol{P}_2,\ \cdots,\ \boldsymbol{P}_n)=\inf(\boldsymbol{r}_i)=\sup(\boldsymbol{a}_i\boldsymbol{Q}_x\boldsymbol{a}_i^{\mathrm{T}}\boldsymbol{P}_i-1) \\ f_3(\boldsymbol{P}_1,\ \boldsymbol{P}_2,\ \cdots,\ \boldsymbol{P}_n) \end{cases} \tag{16}$$

where $\sum_{i=1}^{n}\boldsymbol{P}_i$ =const; $\boldsymbol{P}_i\geq 0$, i=1, 2, ⋯, n. The optimal design is achieved by minimizing the objective functions, and the comprehensive evaluation function can be further expressed as

$$f=(f_1(\boldsymbol{P})-f_1^*)^2+(f_2(\boldsymbol{P})-f_2^*)^2+(f_3(\boldsymbol{P})-f_3^*)^2 \tag{17}$$

where the optimal P_{dop} and reliability values are denoted as f_1^* and f_2^* respectively. The cost constraint f_3^*, which is omitted in our scheme, is based on the system performance and actual requirement, and the minimum value of the assessment gives the optimal solution. Then the comprehensive evaluation function becomes

$$f=\lambda_1(f_1(\boldsymbol{P})-f_1^*)^2+\lambda_2(f_2(\boldsymbol{P})-f_2^*)^2 \tag{18}$$

where f_1^* and f_2^* can also be assigned with different weight coefficients, λ_1 and λ_2. The weights are same when each factor has the same effect on the final optimization scheme.

4.2 Structure optimal design scheme

For a given receiver station, The P_{dop} value only depends on the relative spatial position between the satellites (including PLs) and the receiver, which can be regarded being influenced by azimuth (a), elevation angel (e) and epoch (t) of the satellites. Therefore, a four-dimensional model was established with (a, e, t) as independent variables and P_{dop} as dependent variable to describe the structure of a GNSS/PLs system. Then the system performance can be assessed with P_{dop}:

$$P_{\mathrm{dop}}=f(a,\ e,\ t) \tag{19}$$

where $f(\cdot)$ is a mapping function; $a\in[0^\circ,360^\circ)$; $e\in[-90^\circ,90^\circ]$; $t\geq 0$.

The four-dimensional model shows the value of P_{dop} panoramically and provides theoretical basis for selecting PLs' position. It is not easy to select the optimal positions of PLs according to the above four-dimensional model directly. Considering the practical application, the following technology scheme is presented (Fig. 1).

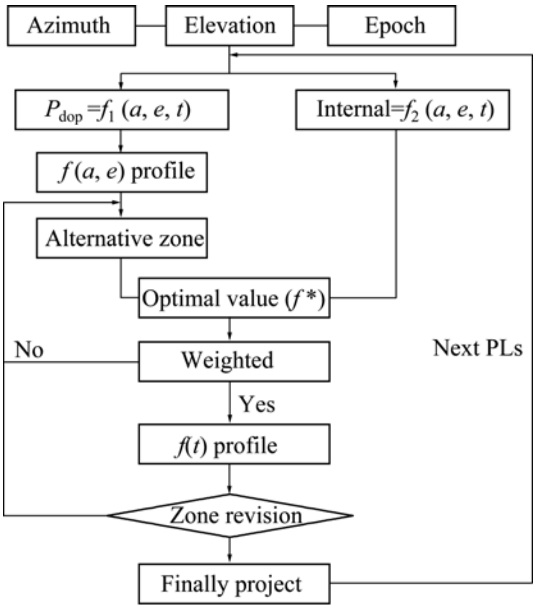

Fig. 1 Technology scheme for PLs optimal design

The practical procedure to determine PLs position is described as follows: Firstly, the profile of P_{dop} along the time axis is intercepted with respect to a certain time interval. Secondly, the optimum zone for PLs is selected as an alternative according to the P_{dop} value. Then, the PLs position can be fixed with Eq. (18) considering the optimum zones and the profile of the reliability value. And if the position is not permitted to install PLs according to the real circumstances, the optimum zone must be re-selected. Finally, the ultimate solution is determined by testing whether the curve of P_{dop} along time axis is smooth. Once the previous PLs were selected, it would be regarded an extra GNSS satellite, and the following PLs selection repeats the same procedure.

In practice, for the limited circumstances, some alternative locations of PLs can be determined in advance, which gets rid of some impossible area and helps to reduce computation burden.

5 Experimental results and analysis

5.1 GPS/PLs structure analysis

In order to examine the performance of the model, an extensive study was conducted on a forced centering apparatus collecting data from two stations in CUMT campus on April 10, 2011 with Trimble R8 receivers. Figure 2 shows the visible satellite distribution at the rove station, named WEST, during the observation period. A 60 min data set was collected at the frequency of 1 Hz. The P_{dop} was used to show the process of comprehensive evaluation of system availability.

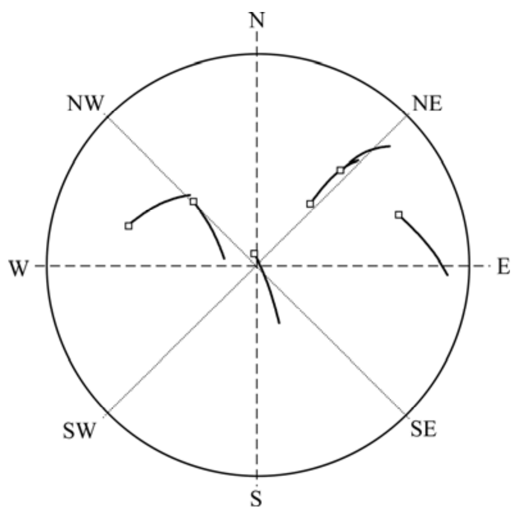

Fig. 2 Distribution of satellites

South of the station WEST was blocked by a certain building with 6 visible satellites. 1000 epochs data in total were utilized for analysis (1 epoch equals 1 s). Figure 3 shows the P_{dop} and internal reliability variations during 1000 epochs without PLs, P_{dop} gradually decrease from 3.6 to 3.3 and internal reliability varies in the range of 8.03−8.17.

The panorama of the P_{dop} variations with one augmented PLs corresponding to elevation angle from −90° to 90° and azimuth angle from 0° to 360° at the 800th epoch is shown in Fig. 4. Figure 5 shows the corresponding internal reliability panorama, the station WEST is set as the center. Obviously, the performance of the system is improved when one PL is joined. The P_{dop} reduces to 2.017−3.319. The black area in Fig. 4 shows a lower P_{dop} result which can reduce to 2.017−2.109, while the red area gets a worse performance. The internal reliability also shows a variability feature due to the diverse location of the added PLs, which varies from 6.279 to 8.076, while the dark blue area shows a better result.

The optimum layout of PLs based on P_{dop} and internal reliability is contradictory, and the single-object evaluation shows its insufficient, so the multi-object

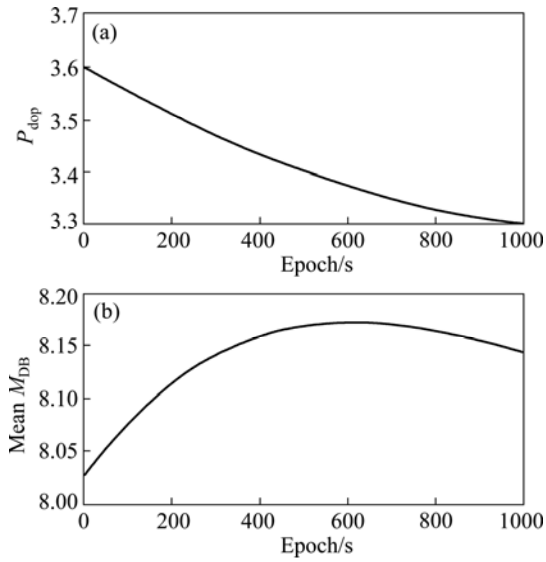

Fig. 3 P_{dop} (a) and internal reliability (b) varying with epoch without PLs

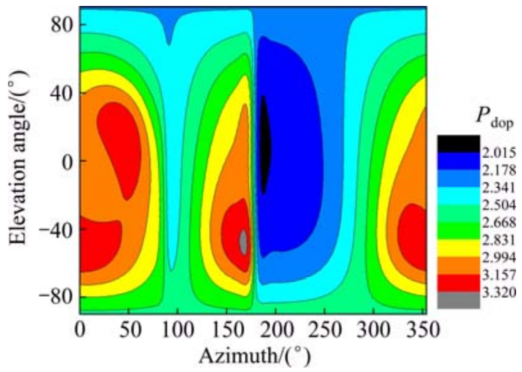

Fig. 4 P_{dop} variations with one PL

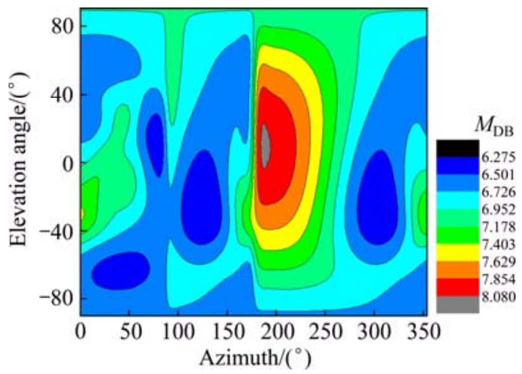

Fig. 5 Internal reliability variations with one PL

evaluation model are considered. Here, the weight coefficient for precision is 0.6 and that of reliability is 0.4. Figure 6 shows the evaluation result. The black area corresponding to azimuth equal to 95° and elevation angle equal to −25° shows the best result where the corresponding P_{dop} is 2.418 and the internal reliability is 6.645. Figure 7 shows the internal reliability variations of different satellites with the optimum layout of PLs.

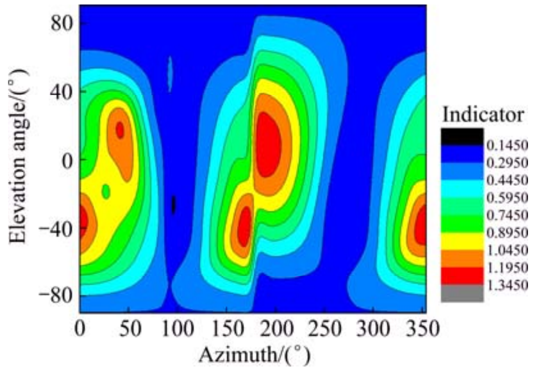

Fig. 6 Comprehensive evaluation indicators with 6 visible satellites

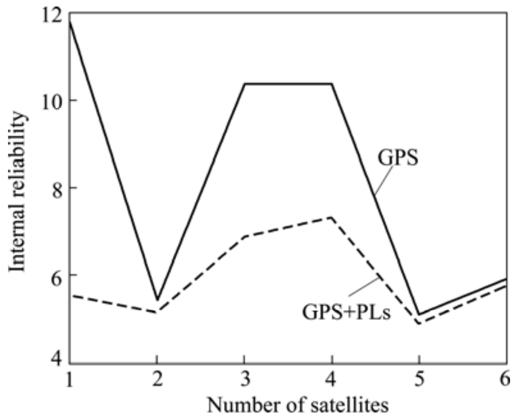

Fig. 7 Internal reliability variations of different satellites

In practical, the real environment should be considered when designing the GNSS/PLs system. When one more PLs are needed in real situation, the previous PL chosen based on multi-object evaluation methods is regarded a GNSS satellite, and the PLs to be added should be chosen in the same procedure. The number of the added PLs is also affected by the cost and actual requirement.

5.2 Real design for open-pit mine

The west open-pit mine of Fushun mining group Co., Ltd., was used to conduct the research [18]. The open-pit mine was 6.6 km long in east-west direction and 2 km wide from north to south, with a total area of 13.2 km^2 and vertical depth of 388 m. Latitude and longitude of the mine were 41.8420° 50.5' N and 123.8840° 53.0' E, respectively. 4 PLs were assumed to locate at the 4 corners of the open-pit mine, the tropospheric error and the random noise were included in the PLs pseudoranges. The simulated GNSS (GPS, Galileo, GLONASS)/PLs system and the simulated moving trajectory of the receiver are shown in Fig. 8. Figure 9 shows the satellite visibility of GNSS during one day.

The D_{op} of the GPS/PLs integration system and the GNSS/PLs integration system at the specific epoch are shown in Table 1, where x-D_{op}, y-D_{op}, V_{dop}, H_{dop} refer to the dilution of precision in x-, y-, vertical and horizontal direction, respectively.

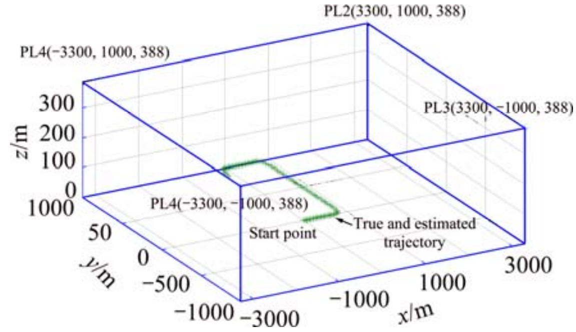

Fig. 8 Simulated moving trajectory

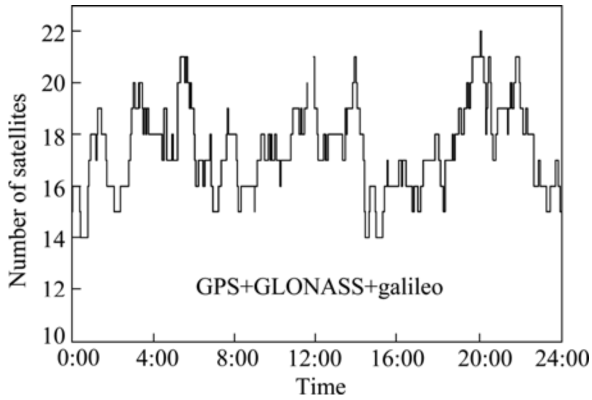

Fig. 9 Satellite visibility of GNSS during one day

Table 1 D_{op} for GPS/PLs system and GNSS/PLs system with different combinations

System	x-D_{op}	y-D_{op}	V_{dop}	H_{dop}	P_{dop}
GPS	0.9675	1.1077	2.6563	1.4707	3.0363
GPS +PL1	0.9665	0.9573	2.0080	1.3604	2.4254
GPS +PL2	0.6519	0.8710	1.5075	1.0879	1.8591
GPS +PL3	0.6524	1.0013	1.6333	1.1951	2.0238
GPS +PL4	0.9614	1.0937	2.2766	1.4562	2.7025
GPS+(PL1+PL2)	0.5510	0.8322	1.2942	0.9981	1.6344
GPS +(PL1+ PL2+PL3)	0.4901	0.8200	1.1819	0.9552	1.5197
GPS +(PL1+PL2+ PL3+PL4)	0.4415	0.8021	1.1206	0.9156	1.4471
GNSS + (PL1+PL2)	0.4415	0.8021	1.1206	0.9156	1.4471
GNSS + (PL1+PL2+PL3)	0.4084	0.5317	0.7992	0.6704	1.0431
GNSS +(PL1+ PL2+PL3+PL4)	0.3762	0.5251	0.7494	0.6460	0.9894

Table 1 shows clearly that the D_{op} decreases with an increase in PLs' number, especially in vertical direction. It is obvious that the augmentation can significantly improve the geometric strength of the positioning solutions and availability. It also shows that different location of PLs differs the D_{op} value. PL_2 and PL_3 provide better D_{op} which indicates better PLs location. As expected, the more PLs we have, the better D_{op} value can be achieved, and the GNSS/PLs system generates better results for the better geometric strength and more visible satellites, which is very helpful in certain extreme conditions.

The internal reliability and external reliability with respect to different satellite numbers of the GNSS/PLs integration system are shown in Fig. 10. It shows the system gets a better reliable test statistics when the PLs are added, which indicates that a better performance can be achieved with the augmentation of PLs, and the more PLs have been added, the better result we get to some extend.

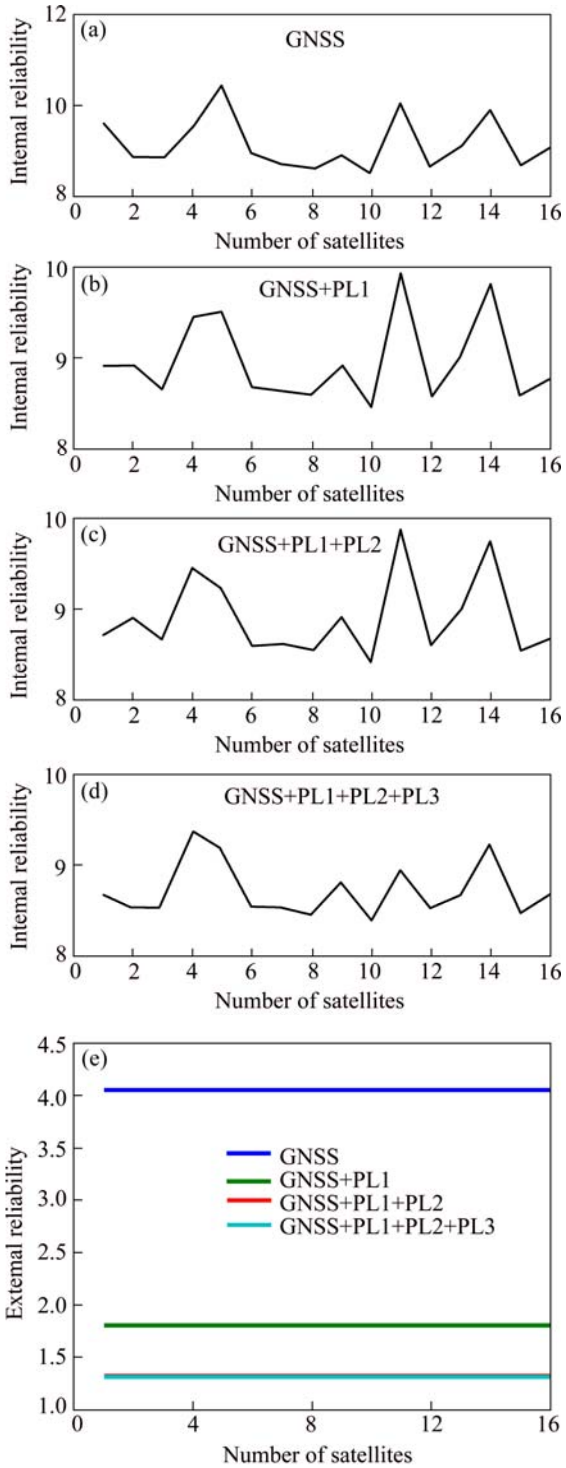

Fig. 10 Internal reliability (a, b, c, d) and external reliability (e) variations for different satellites

In order to investigate the system structure variations, the D_{op} values of the moving trajectory of two schemes are designed: scheme I, the GNSS only system; scheme II, the GNSS/PLs integration system (PL1 is added). H_{dop} and V_{dop} are both calculated to compare the navigation performance.

Figure 11 shows that the integration system (dotted line) gets a better result during the navigation span with the navigation performance improved gradually, where lines 1,2,5 represent the P_{dop}, V_{dop}, H_{dop} corresponding to the scheme I and line 3,4,6 describe the value in scheme II, and the V_{dop} gets a greater improvement than H_{dop}. The improvement becomes more significant when the receiver reaches the edge (after the 88th epoch).

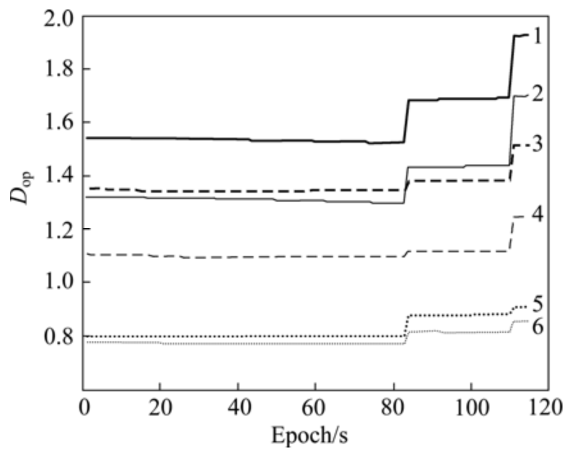

Fig. 11 D_{op} variations of two schemes

The mean M_{DB} during the navigation period is given in Fig. 12. Lines 1,2,3 in Fig.12 give the mean M_{DB} value, horizontal M_{DB} value and vertical M_{DB} value for scheme I respectively and lines 4,5,6 exhibit the corresponding

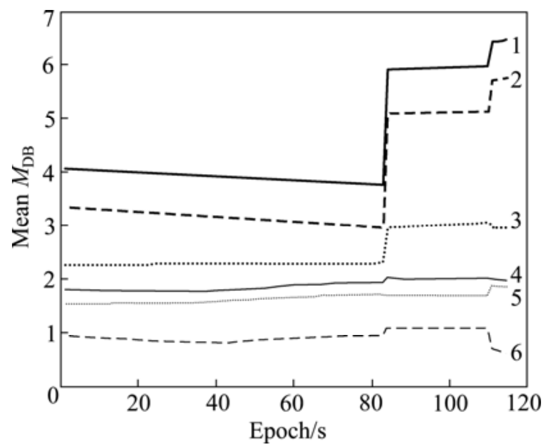

Fig. 12 Mean M_{DB} variations

values for scheme II. It is obviously shown that the GNSS/PLs integration system can achieve better internal reliability and external reliability, and the improvement is caused by adding PLs which dramatically changes the height positioning quality of the integration system.

Considering the multi-objective optimization case, the P_{dop} and external reliability, M_{DB}, are chosen as the constraints with different weight coefficients. The weight coefficients are determined as 0.4 for D_{op} and 0.6 for M_{DB}. Figure 13 gives the comprehensive result of the system.

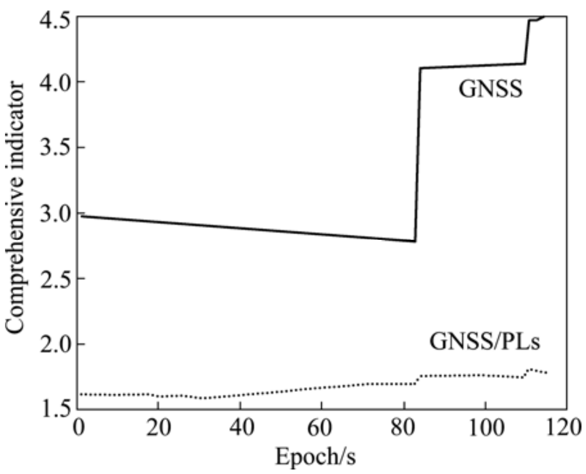

Fig. 13 Comprehensive indicator variations

6 Conclusions

1) The optimum deployment of PLs for GNSS/PLs integration system was investigated. Dilution of precision and reliability (internal reliability and external reliability) are two important factors to evaluate the positioning performance.

2) The weight scheme of different functions is assigned for experience, which may lead to nonoptimal design. Therefore, future research should pay more attention to multi-object weight assignment, and comprehensive evaluation functions should be investigated.

References

[1] KIM D, RICHARD B, LANGLEY J B. Local deformation monitoring using GPS in an open pit mine: Initial study [J]. GPS Solutions, 2003, 7: 176−185.

[2] WANG Jian-peng, GAO Jing-xiang, LIU Chao, WANG Jian. High precision slope deformation monitoring model based on the GPS/pseudolites technology in open-pit mine [J]. Mining Science and Technology, 2010, 20(1): 126−132.

[3] ZUO Ming, DU Jun-ping. Satellite positioning and dispatch system of vehicles and mine equipment in open-pit mines [J]. Metal Mine, 2007(6): 51−54. (in Chinese)

[4] GU Qing-hua, LU Cai-wu, GUO Jin-ping, JING Shi-qun. Dynamic management system of ore blending in an open pit mine based on GIS/GPS/GPRS [J]. Mining Science and Technology, 2010, 20(1): 132−137.

[5] ZHENG Guo-zhong, XU Jia-mo, MA Feng-shan, CAO Jing, XIA Yi, ZHENG Shi-lin. GPS monitoring of slope deformation in Jinchuan open pit mine [J]. Journal of Engineering Geology, 1998, 6(3): 282−288. (in Chinese)

[6] GAO Jing-xiang, LIU Chao, WANG Jian, LI Zeng-ke, MENG Xiang-chao. A new method for mining deformation monitoring with GPS-RTK [J]. Transactions of Nonferrous Metals Society of China, 2011, 21: s659−s664.

[7] WANG Bin, WANG Chun-yi. Application study on WIFI wireless location technology in open pit [J]. Metal Mine, 2011(7): 123−126. (in Chinese)

[8] LIU Chao, GAO Jing-xiang, WANG Jian, LIU Yan. GPS/pseudolites technology for the slope deformation monitoring in open-pit mine [J]. Journal of China Coal Society, 2010, 35(5): 755−759. (in Chinese)

[9] BARNES J, RIZOS C, WANG J, SMALL D, VOIGT G, GAMBALE N. Locata: The positioning technology of the future [C]//Proceedings of the 6 th International Symposium on Satellite Navigation Technology including Mobile Positioning & Location Services. Melbourne, Australia, 2003: 49−62.

[10] COBB H S. GPS psedolites: Theory, design and application [D]. California: Department of aeronautics and astronautics, Stanford University, 1997: 87−101.

[11] CROSS P A, HAWKSBEE D J, NICOLAI R. Quality measures for differential GPS positioning [J]. The Hydorgraphic Journal, 1994, 72: 17−22.

[12] LI B H, AEMPSTER A G, WANG J. 3D DOPs for positioning applications using range measurements [J]. Wireless Sensor Network, 2011, 3(10): 334−340.

[13] HEWITSON S. Quality control for integrated GNSS and inertial navigation systems [D]. Sydney: School of Surveying and Spatial Information Systems, the University of New South Wales, 2006: 55−59.

[14] BAARDA W. A testing procedure for use in geodetic networks [M]. Delft: Netherlands Geodetic Commission, 1968: 97.

[15] LEE H B. A novel procedure for assessing the accuracy of hyperbolic multilateration system [J]. IEEE Trans Aerosp Electron Syst, 1975, 11(1): 2−15.

[16] XU Pei-liang. Multi-objective optimal second order design of networks [J]. Bulletin Geod, 1989, 63: 297−308.

[17] WANG Jian, JIANG Kun, LI Bing-hao. Optimizing pseudolites struc ture for GPS/PLs relative positioning [C]//International Global Navig ation Satellite Systems Society, IGNSS Symposium 2011. Sydney, Australia: University of New South Wales, 2011: 15−17.

[18] LIU Wen-long, WANG Jian, ZHAO Xiao-ping. Reliability of PL-enhanced GNSS navigation system [J]. Bulletin of Surveying and Mapping, 2009(6): 5−8. (in Chinese)

露天矿定位的 GNSS/伪卫星结构优化模型

单正英[1]，韩厚增[2]，姜 昆[2]

1. 重庆大学 土木工程学院，重庆 400030；
2. 中国矿业大学 国土环境与灾害监测国家测绘地理信息局重点实验室，徐州 221116

摘 要：提出新的露天矿 GNSS/伪卫星组合定位系统的结构优化模型。通过引入空间位置精度因子(P_{dop})与可靠性作为优化指标，建立多目标优化模型用于选择伪卫星的最优位置。在考虑实际环境的情况下，建立以方位角(a)、高度角(e)和历元(t)为自变量，P_{dop}为因变量的四维模型，并用于最优伪卫星布设带的选择。通过分析 P_{dop}随时间的变化特征，最终确定最优的伪卫星布设位置。利用中国矿业大学校园内实测的天宝 R8 GPS 数据测试模型的有效性，评价系统结构指标的变化规律，并将该模型用于抚顺矿业集团的西露天矿 GNSS/伪卫星系统布设试验。通过模型优化可在降低成本的同时提高集成系统的整体性能，分析表明 P_{dop}与可靠性都得到了有效提高。

关键词：露天矿；精度因子；可靠性；GNSS/伪卫星系统；优化

(Edited by Hua YANG)